



Research Paper

ON THE DISTRIBUTION GENERATED BY WARING-TYPE PROBABILITY WITH APPLICATION TO COVID-19 DATA

DAVOOD FARBOD ¹

¹Department of Mathematics, Faculty of Engineering Science, Quchan University of Technology, Quchan, Iran,
d.farbod@qiet.ac.ir

ARTICLE INFO

Article history:

Received: 26 December 2024

Accepted: 26 July 2025

Communicated by Nasrin Eghbali

Keywords:

Asymptotic properties

COVID-19

Maximum likelihood

Rival models

Waring-type probability

MSC:

62F12; 60E05; 62F10; 62P10

ABSTRACT

Farbod (2024) [9] introduced a 2-parameter regularly varying discrete distribution generated by Waring-type probability (2-RDWP). In this paper, asymptotic properties of maximum likelihood estimators of the unknown parameters are established for the 2-RDWP model. Some new plots including cumulative distribution function, survival function and hazard rate function are illustrated for the 2-RDWP model. Two real data sets of COVID-19 are applied to show the model's applicability compared to other rival distributions. Based on some statistical criteria we see that the 2-RDWP, for these real data sets, has satisfactory results with respect to rival models. Using an optimization algorithm, maximum likelihood estimations of the unknown parameters are proposed.

1. INTRODUCTION

Recently, a new 2-parameter regularly varying discrete distribution generated by Waring-type probability (in short, we call 2-RDWP) was introduced by Farbod in 2024 [9] for the needs of bioinformatics and biomolecular systems. Also, some mathematical and statistical properties, and application of the 2-RDWP were given by Farbod [9]. We notice that many

*Address correspondence to Davood Farbod; Department of Mathematics, Faculty of Engineering Science, Quchan University of Technology, Quchan, Iran, E-mail: d.farbod@qiet.ac.ir.

discrete distributions have been proposed based on different methods for bioinformatics and biological needs (see, for example, [2, 3, 14]).

The motivation for writing this paper is to establish large-sample properties of the maximum likelihood (ML) estimators of the 2-RDWP model. In addition, due to the great applicability of the discrete distributions in analyzing count data, we shall attempt to model 2-RDWP distribution with different coronavirus disease-19 (COVID-19) data sets. In the sequel, based on two real data sets and using well-known statistical criteria, the advantages of our model over some other competitive models are provided. ML estimations of the unknown parameters for our model and also competitive models are given.

We consider the following function [7]

$$(1.1) \quad p_x(\alpha) = \frac{(r+x-1)^{r+x-1}}{(q+x)^{q+x}}, \quad x > 0.$$

From (1.1) and using discretization, the probability mass function (PMF) of 2-RDWP has been introduced as follows [7]:

$$(1.2) \quad g_x(\alpha) = (d(\alpha))^{-1} \times \frac{(r+x-1)^{r+x-1}}{(q+x)^{q+x}},$$

where $x = 1, 2, \dots$, and $d(\alpha)$ is the *normalization factor (normalization constant)* given by

$$d(\alpha) = \sum_{y=1}^{\infty} \frac{(r+y-1)^{r+y-1}}{(q+y)^{q+y}}$$

and $\alpha = (r, q)$. We note that r and q are the unknown parameters ($r > 0$ and $r < q$). The function (1.2) is a probability function and is considered as a PMF on the set of positive integers $x \in \mathbb{N}_+ = \{1, 2, 3, \dots\}$. Moreover, the model $g_x(\alpha)$ (1.2) varies regularly at infinity with exponent $(-\rho)$ having [9]

$$(1.3) \quad -\rho = -(q+1-r) < -1.$$

This paper investigates some statistical properties and also propose real applications of the 2-RDWP model (1.2).

The structure of this document is as follows. In Section 2, we present large-sample properties of the ML estimators of the 2-RDWP's unknown parameters. Section 3 considers some plots for cumulative distribution function (CDF), survival function (SF) and hazard rate function (HRF). Section 4 proposes applications of the model and compares it with rival models. Also, ML estimations of the unknown parameters are given in Section 4. A conclusion is provided in Section 5. An Appendix is proposed which contains the PMFs of some rival models.

2. ASYMPTOTIC PROPERTIES

This section establishes the asymptotic properties of the ML estimators of unknown parameters. In other words, the ML estimator's consistency, asymptotic normality, asymptotic efficiency and asymptotic unbiasedness are established. Compared to Farbod [6], it suffices

to prove that the family of $g_x(\alpha)$ holds in some regularity conditions (RCs). Assume that $\Theta = \{\alpha = (r, q), 0 < r < q\}$ is a parametric space such that $\Theta \subset \mathbb{R}^2$ and $X_n = (X_1, \dots, X_n)$ is a random variable with realization $x_n = (x_1, \dots, x_n)$. The notation n is the sample size. We state the RCs for the model (1.2). Before that, let us obtain derivatives for $p_x(\alpha)$ function.

2.1. Derivatives. In this part, let us obtain the first and second derivatives of $p_x(\alpha)$ (1.1) with respect to parameters (r, q) , which are used in the sequel. The first and second derivatives of $p_x(\alpha)$ (1.1) are given as follows:

$$(2.1) \quad \frac{\partial p_x(\alpha)}{\partial r} = (\ln(r+x-1) + 1) \frac{(r+x-1)^{r+x-1}}{(q+x)^{q+x}}$$

$$(2.2) \quad \frac{\partial p_x(\alpha)}{\partial q} = -(\ln(q+x) + 1) \frac{(r+x-1)^{r+x-1}}{(q+x)^{q+x}}$$

$$(2.3) \quad \frac{\partial^2 p_x(\alpha)}{\partial r^2} = \left(\frac{1}{r+x-1} + (\ln(r+x-1) + 1)^2 \right) \frac{(r+x-1)^{r+x-1}}{(q+x)^{q+x}}$$

$$(2.4) \quad \frac{\partial^2 p_x(\alpha)}{\partial q^2} = \left(-\frac{1}{q+x} + (\ln(q+x) + 1)^2 \right) \frac{(r+x-1)^{r+x-1}}{(q+x)^{q+x}}$$

$$(2.5) \quad \frac{\partial^2 p_x(\alpha)}{\partial r \partial q} = \frac{\partial^2 p_x(\alpha)}{\partial q \partial r} = -\left((\ln(q+x) + 1)(\ln(r+x-1) + 1) \right) \frac{(r+x-1)^{r+x-1}}{(q+x)^{q+x}}$$

2.2. RCs. Let us state RCs 1-5 conditions and establish them for the model (1.2).

RC 1. There exists a compact subset \bar{S} of the parametric set Θ , which contains the open neighborhood of a true value α_0 of the parameter α .

RC 2. The distribution with PMF $g_x(\alpha)$ has common support; that is, the set $\text{Support} \{x : g_x(\alpha) > 0\}$ does not depend on α .

RC 3. For all $\alpha \in \Theta$ and for all $\alpha_0 \in \bar{S}$ ($\alpha \neq \alpha_0$), the condition $\sum_{x=1}^{\infty} |g_x(\alpha) - g_x(\alpha_0)| > 0$ is satisfied.

RC 4. The function $\ln g_x(\alpha)$ is twice continuously differentiable by α and there exists a function $D(x)$ such that

$$D(x; \alpha) = \left| \frac{\partial^2 \ln g_x(\alpha)}{\partial \alpha_i \partial \alpha_j} \right| \leq D(x), \quad i, j = 1, 2; \quad \alpha_1 = r, \quad \alpha_2 = q,$$

for which $E_\alpha[D(X)] < \infty$.

RC 5. Fisher's information matrix is given by

$$\mathbf{I}(\alpha) = ||I_{ij}(\alpha)||, \quad i, j = 1, 2,$$

where $I_{ij}(\alpha) = -E \left[\frac{\partial^2 \ln g_x(\alpha)}{\partial \alpha_i \partial \alpha_j} \right]$ is a positive definite continuous function for all $\alpha \in \bar{S}$ such that $|\mathbf{I}(\alpha)| \equiv \det \mathbf{I}(\alpha) > 0$.

The proofs RC 1, RC 2 and RC 3 are met, obviously and the details are avoided. Let us prove RC 4 and RC 5.

Proof of RC 4. The second derivatives of $\ln g_x(\alpha)$ by r and q are given by:

$$(2.6) \quad \frac{\partial^2 \ln g_x(\alpha)}{\partial r^2} = \frac{1}{p_x(\alpha)} \frac{\partial^2 p_x(\alpha)}{\partial r^2} - \left(\frac{1}{p_x(\alpha)} \frac{\partial p_x(\alpha)}{\partial r} \right)^2 - \frac{\partial}{\partial r} \left(\frac{1}{d(\alpha)} \frac{\partial d(\alpha)}{\partial r} \right)$$

$$(2.7) \quad \frac{\partial^2 \ln g_x(\alpha)}{\partial q^2} = \frac{1}{p_x(\alpha)} \frac{\partial^2 p_x(\alpha)}{\partial q^2} - \left(\frac{1}{p_x(\alpha)} \frac{\partial p_x(\alpha)}{\partial q} \right)^2 - \frac{\partial}{\partial q} \left(\frac{1}{d(\alpha)} \frac{\partial d(\alpha)}{\partial q} \right)$$

$$(2.8) \quad \frac{\partial^2 \ln g_x(\alpha)}{\partial r \partial q} = \frac{\partial^2 \ln g_x(\alpha)}{\partial q \partial r} = \left(\frac{1}{p_x(\alpha)} \frac{\partial^2 p_x(\alpha)}{\partial q \partial r} \right) - \left(\frac{1}{p_x(\alpha)} \frac{\partial p_x(\alpha)}{\partial r} \right) \left(\frac{1}{p_x(\alpha)} \frac{\partial p_x(\alpha)}{\partial q} \right) - \frac{\partial}{\partial q} \left(\frac{1}{d(\alpha)} \frac{\partial d(\alpha)}{\partial r} \right)$$

Using (2.1)-(2.5) and (2.6)-(2.8) and for sufficiently large x , after some simplifications we get

$$(2.9) \quad D(x) = O(\ln^4 x),$$

where the symbol O is called big O notation and defined by Bachmann-Landau.

It follows from (2.9) that $E_\alpha[D(X)] < \infty$. The proof of RC 4 is finished.

Proof of RC 5. Based on the definition of Fisher's information matrix and from Lemmas proposed by Farbod [9, Lemma 5.2, Lemma 5.3] (for $n = 1$), this condition is verified.

Let $l(X_n; \alpha) = \ln L(X_n; \alpha) = \ln \prod_{i=1}^n g_{x_i}(\alpha)$ be the logarithm of likelihood function. Compared to Borovkov [4] and from the RCs 1-5, the following results are concluded.

Theorem 2.1. Suppose that $\alpha_0 = (r_0, q_0) \in \bar{S}$ is the true value of $\alpha = (r, q)$, and the conditions RCs 1-5 are met. Under these conditions, with probability tending to one when n tends to infinity, there exists a solution $\hat{\alpha}_n = (\hat{r}_n, \hat{q}_n)$ of the system of likelihood equations

$$\frac{\partial l(X_n; \alpha)}{\partial r} = 0, \quad \frac{\partial l(X_n; \alpha)}{\partial q} = 0,$$

such that:

(a) $\hat{\alpha}_n$ is a consistent estimator for α , namely $\hat{\alpha}_n \xrightarrow{P} \alpha$ as $n \rightarrow \infty$ (\xrightarrow{P} means convergence in probability).

(b) $\hat{\alpha}_n$ is an asymptotic normal and asymptotic efficient estimator for α , namely

$$(2.10) \quad u_n = \sqrt{n}(\hat{\alpha}_n - \alpha) \xrightarrow{d} u \sim N(\mathbf{0}, \mathbf{I}^{-1}(\alpha)),$$

where $u \sim N_2(\mathbf{0}, \mathbf{I}^{-1}(\alpha))$ is a 2-dimensional normal distributed random vector with (vector) mean $\mathbf{0}$ and variance-covariance matrix $\mathbf{I}^{-1}(\alpha)$ (\xrightarrow{d} means convergence by distribution).

(c) there is the convergence of arbitrary order moments of u_n to the respective order moments of u , namely

$$E[u_n^t] \longrightarrow E[u^t], \text{ for all } t \geq 1,$$

in particular, if $t = 1$, then the asymptotic unbiasedness property hold

$$E[\hat{\alpha}_n] = \alpha + o\left(\frac{1}{\sqrt{n}}\right), \text{ the symbol } o, \text{ called small } o \text{ notation}$$

and also for sufficiently large n

$$E\left[(\hat{\alpha}_n - \alpha)^T(\hat{\alpha}_n - \alpha)\right] = \frac{1}{n} \cdot \mathbf{I}^{-1}(\alpha) + o\left(\frac{1}{n}\right),$$

where $(.)^T$ is a transpose vector.

3. FIGURES

Farbod [9] illustrated some plots for the PMF of 2-RDWP model. In this section, we plot the CDF, SF and HRF of 2-RDWP for some values of parameters. For the model (1.2), the CDF is proposed by [9]

$$(3.1) \quad F_x(\alpha) = P(X \leq x) = (d(\alpha))^{-1} \sum_{m=1}^x \frac{(r+m-1)^{r+m-1}}{(q+m)^{q+m}}$$

and the SF is given by $\bar{F}_x(\alpha) = 1 - F_x(\alpha)$ and HRF is given by $h_x(\alpha) = \frac{g_x(\alpha)}{\bar{F}_x(\alpha)}$.

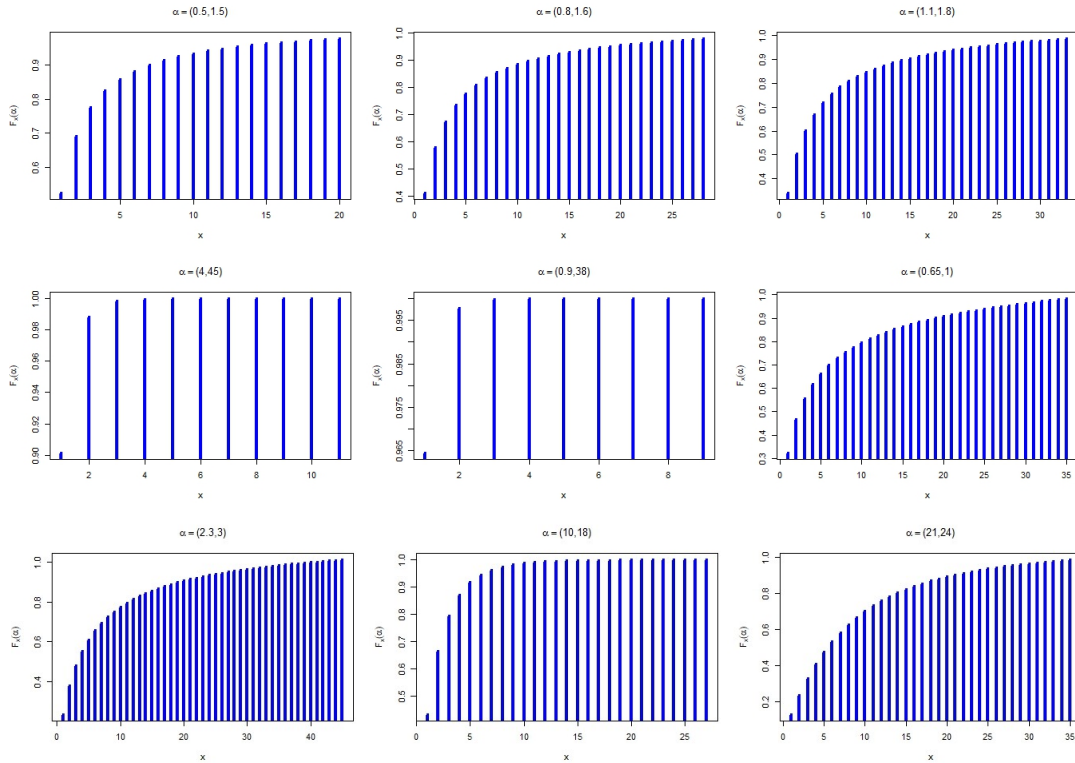


FIGURE 1. Plot of CDF for the model (1.2) for different parameters values

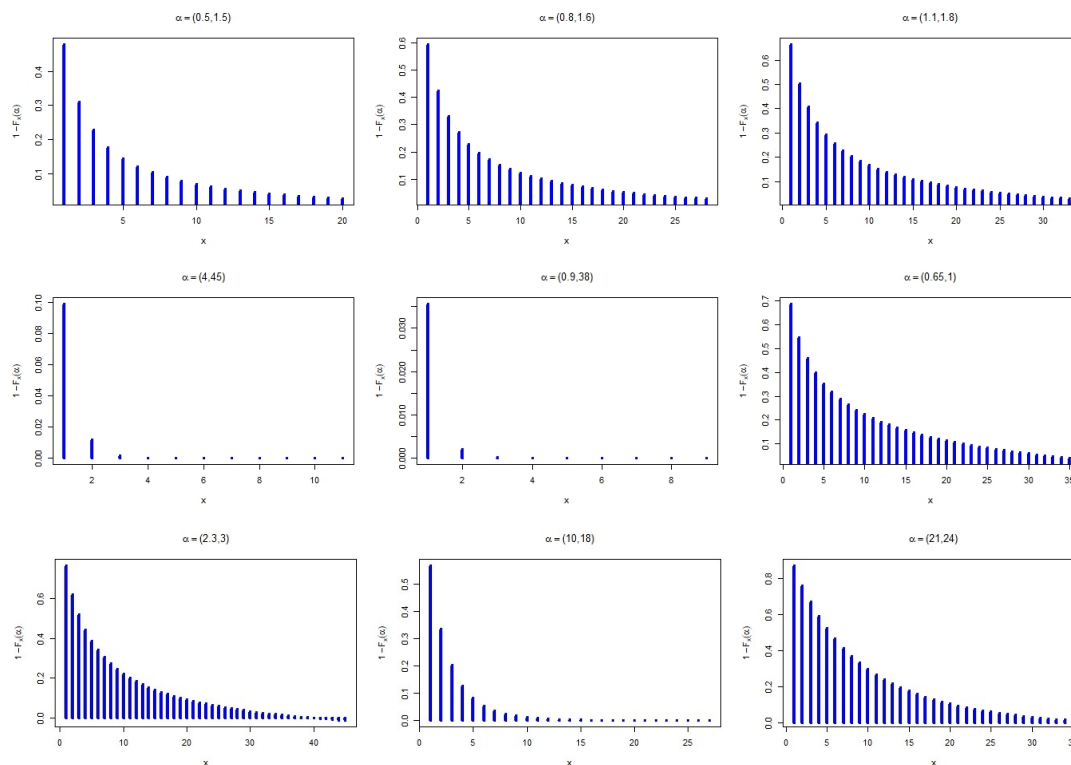


FIGURE 2. Plot of SF for the model (1.2) for different parameters values

4. APPLICATIONS TO COVID-19 DATA AND COMPARISON

As it was proved by Farbod [9], the 2-RDWP model (1.2) has been introduced for the needs of phenomena arising in bioinformatics, biosystems, etc. Farbod [9] fitted the model with a real data set in bioinformatics and then compared it with some models. The purpose of this research is to show the empirical importance of the 2-RDWP model with other real data sets on COVID-19 and also compare it with some rival models.

Compared to Farbod [9], computational problems have been arisen for large values x . To solve this computational problem, our PMF (1.2) can be considered as [9]:

$$(4.1) \quad g_x^*(\alpha) = \left(\sum_{y=1}^{\infty} \frac{\left(1 + \frac{r-1}{y}\right)^y (y+r-1)^{r-1}}{\left(1 + \frac{q}{y}\right)^y (y+q)^q} \right)^{-1} \cdot \frac{\left(1 + \frac{r-1}{x}\right)^x (x+r-1)^{r-1}}{\left(1 + \frac{q}{x}\right)^x (x+q)^q}.$$

Remark 1. It is obvious that the PMF (1.2) equals the PMF (4.1) [9]. Therefore, for numerical and computational aims, we need to consider the PMF (4.1).

4.1. Real examples. COVID-19 was reported in December 2019 in Wuhan, China, and within some months spread like a pandemic around the world. The WHO described COVID-19 as a pandemic in March 2020. Countries around the world have increased their efforts to decrease the COVID-19 spread rate. For details about this disease, see [18]. Here, let us consider two real data sets in COVID-19. These data sets are collected from the *World Health Organization (WHO)* [17] coronavirus infection and *Statista* [19] (German online platform that specializes in data gathering and visualization).

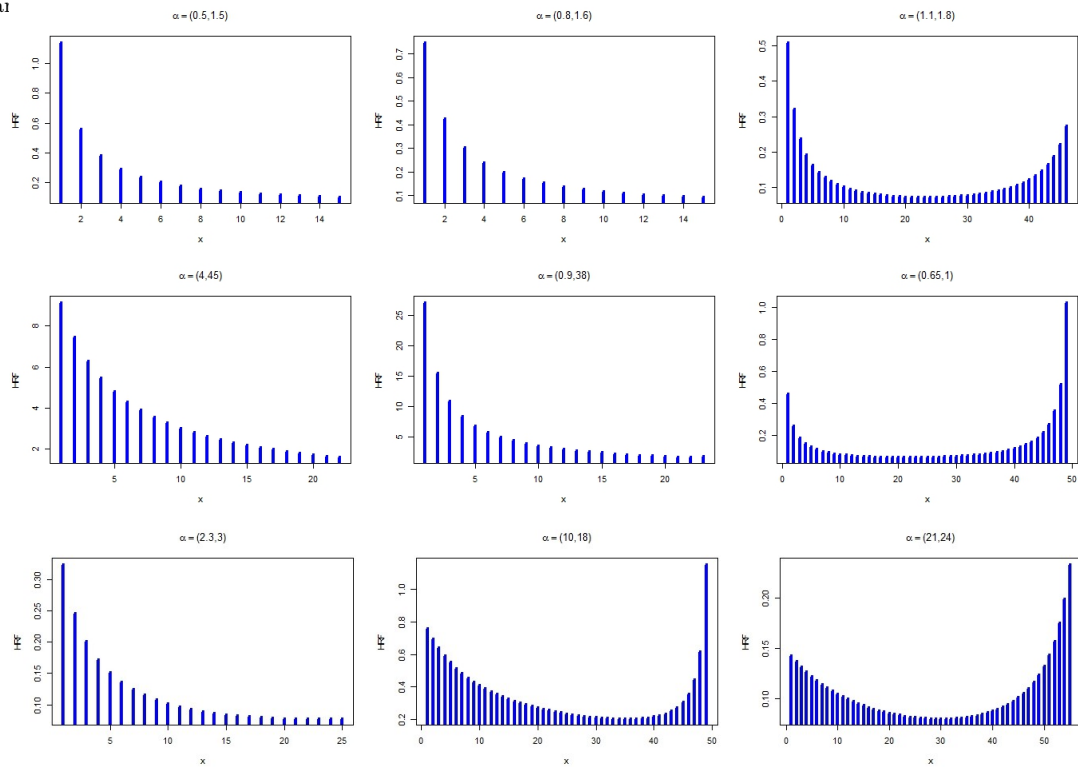


FIGURE 3. Plot of HRF for the model (1.2) for different parameters values. The HRF can be decreasing and bathtub-shaped depending on its parameters values.

TABLE 1. A data set of COVID-19 in different countries for seven days. The data consists of the number of deaths reported in seven days of infection (March 2023)

x	1	2	3	4	5	6	7	8	9	10
frequency	8	5	4	1	1	2	1	1	1	2
x	11	12	14	15	16	17	19	21	22	29
frequency	2	2	2	1	1	1	2	1	1	1
x	35	45	59	63	70	74	75	80	83	92
frequency	1	1	1	1	1	1	1	1	1	1
x	129	139	273	315	433	1251	1887			
frequency	1	1	1	1	1	1	1			

Example 4.1. Let us have a data set of COVID-19 in different countries for seven days. The data consists of the number of deaths reported in seven days of infection (March 2023). The data are given in Table 1 [17].

Table 2 presents descriptive statistics for the data from Example 4.1. From Table 2, the value of skewness is equal to 5.303. It means that the data has positive skewness.

TABLE 2. Descriptive statistics for the data from Example 4.1

n	Min	Q1	Median	Mean	Variance	Q3	Max	Skewness	Kurtosis
64	1	3	14.5	89.734	80599.055	58	1887	5.303	29.834

TABLE 3. A data set of COVID-19 in different countries Coronavirus (COVID-19) deaths worldwide per one million population as of July 13, 2022, by country

x	1	2	3	4	5	6	7	8	9	10
frequency	14	4	7	4	5	3	1	2	2	3
x	11	12	13	14	15	16	17	18	20	21
frequency	3	3	2	2	1	3	1	1	2	2
x	22	29	30	31	32	33	35	36	37	40
frequency	1	1	1	1	1	1	1	1	1	1
x	42	43	63	65	66	78	97	117	118	120
frequency	2	1	1	1	1	1	1	1	1	1
x	121	123	127	132	153	171	247	249	301	302
frequency	1	1	1	2	1	1	1	1	1	1
x	312	321	465	620	692	715	1673	3418		
frequency	1	1	1	1	1	1	1	1		

Example 4.2. Let us consider a data set of COVID-19 deaths (deaths in 7 days) worldwide per one million population as of July 13, 2022, by country. The data consists of the number of deaths reported in seven days. The data are given in Table 3 [19].

Table 4 presents descriptive statistics for the data from [Example 4.2](#). From Table 4, the value of skewness is equal to 6.918. It means that the data has positive skewness.

TABLE 4. Descriptive statistics for the data from [Example 4.2](#)

n	Min	Q1	Median	Mean	Variance	Q3	Max	Skewness	Kurtosis
105	1	4	13	113.5810	148542.900	64	3418	6.918	54.841

4.1.1. *Comparison based on statistical criteria.* It is of interest to obtain some statistical criteria for our 2-RDWP model and then compare it with five rival models.

Akaike information criterion (AIC) is proposed by [1]

$$AIC = 2 \ln L + 2k$$

where k the number of parameters in the model and $-\ln L$ is the maximized value of the likelihood function for the estimated distribution.

Note. The AIC is a mathematical method for evaluating how well a model fits the data it was generated from. In statistics, AIC is used to compare different possible models and determine which one is the best fit for the data. AIC was introduced in 1973 by Hirotugu Akaike as an extension to the maximum likelihood principle. Maximum likelihood is conventionally applied to estimate the parameters of a model once the structure and dimension of the model have been formulated. Akaike's idea was to combine into a single procedure the process of estimation with structural and dimensional determination. For details about AIC, we refer the readers to [1, 5].

AIC with corrected (AICc) is presented by [5]

$$AICc = AIC + \frac{2k^2 + 2k}{n - k - 1}$$

where n is the sample size; Bayesian information criterion (BIC) is given by [5, 15]

$$BIC = -2 \ln L + k \ln n$$

Hannan-Quinn information criterion (HQIC) is given by [5, 12]

$$HQIC = -2 \ln L + 2k \ln(\ln n)$$

and p-value, we compare the 2-RDWP (4.1) with other distributions arising in biosystems, such as the one-parameter skewed discrete Levy distribution (DLD) (5.1) [7], one-parameter skewed Power-Law (PL) model (5.2) [13], one-parameter truncated discrete Cauchy stable distribution (T-DCD) (5.3) [10], one-parameter truncated skewed discrete stable distribution (T-SDSD) (5.4) [8], and two-parameter truncated skewed discrete stable distribution (T-2SDSD) (5.5) [8], all having support on the set of positive integers, i.e. $x \in \mathbb{N}_+ = \{1, 2, 3, \dots\}$.

With the help of new codes in *R statistical software*, we present our results in Tables 5 and 6. It may be seen from Tables 5 and 6 that the 2-RDWP model has the smallest $-\ln L$, AIC, AICc, BIC, HQIC, and the largest p-value. So, for both real data sets, it can be concluded that the 2-RDWP distribution has the best results among compared distributions (DLD, PL, T-DCD, T-SDSD and T-2SDSD models). Also, for instance, for informal goodness of fit tests, we plot the Empirical CDF (ECDF) and fitted CDF of the data set of Table 1 in Figure 4. The PMFs of DLD, PL, T-DCD, T-SDSD and T-2SDSD are given in Appendix.

TABLE 5. Comparing results for 2-RDWP, DLD, PL, T-DCD, T-SDSD and T-2SDSD models for data of Example 4.1, $n = 64$

Model	$\ln L$	k	AIC	AICc	BIC	HQIC	p-value
2-RDWP	-299.3526	2	602.7052	602.9019	607.0229	604.4062	0.653
DLD	-301.6958	1	605.3916	605.4561	607.5505	606.2421	0.08535
PL	-304.1313	1	610.2626	610.3271	612.4215	611.1131	0.01534
T-DCD	-304.9313	1	611.8626	611.9271	614.0215	612.7131	0.2335
T-SDSD	-301.89125	1	605.7825	605.84702	607.9414	606.6329	0.08844
T-2SDSD	-300.6611	2	605.3222	605.5189	609.6399	607.0232	0.3802

TABLE 6. Comparing results for 2-RDWP, DLD, PL, T-DCD, T-SDSD and T-2SDSD models for data of Example 4.2, $n = 105$

Model	$\ln L$	k	AIC	AICc	BIC	HQIC	p-value
2-RDWP	-502.9532	2	1009.9064	1010.0240	1015.2143	1012.0573	0.2496
DLD	-506.3741	1	1014.7482	1014.7870	1017.4022	1015.8236	0.06222
PL	-510.5688	1	1023.1376	1023.2021	1025.7916	1024.2130	0.00048
T-DCD	-515.6864	1	1033.3728	1033.4373	1036.0268	1034.4482	0.03369
T-SDSD	-506.8321	1	1015.6642	1015.7287	1018.3182	1016.7396	0.00966
T-2SDSD	-504.7433	2	1013.4866	1013.6833	1018.7945	1015.6375	0.1171

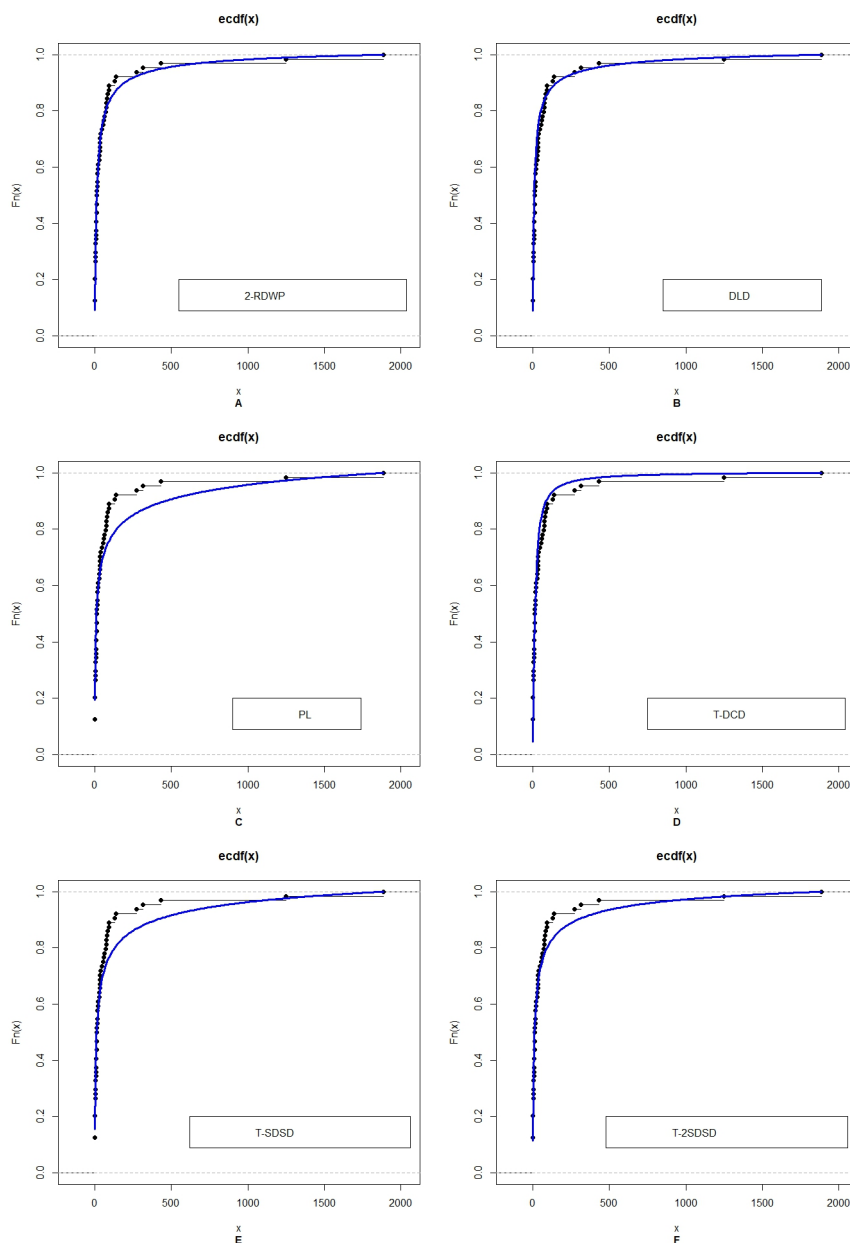


FIGURE 4. Fitting of the data of Table 1 for the models 2-RDWP, DLD, PL, T-DCD, T-SDSD and T-2SDSD.

4.1.2. *ML estimations.* Here, based on two real data sets in Tables 1 and 3, we would like to obtain ML estimations (\hat{r}, \hat{q}) of the unknown two parameters (r, q) . Due to complexity of models, we need to consider numerical and simulation methods. Let us apply limited-memory Broyden-Fletcher-Goldfarb-Shanno for bound-constrained optimization (L-BFGS-B) method [16].

In addition to 2-RDWP model, let us consider rival models including: one-parameter DLD (5.1), one-parameter PL (5.2), one-parameter T-DCD (5.3), one-parameter T-SDSD (5.4), and two-parameter T-2SDSD (5.5). Using L-BFGS-B method and for all mentioned models, we obtain ML estimations and standard errors (SEs) of the unknown parameters.

For the data of Table 1, the results are given in Table 7.

For the data of Table 3, the results are given in Table 8.

TABLE 7. ML estimations of the parameters and the corresponding SEs for the fitted models and for the data from [Example 4.1](#)

	ML estimations	SEs
2-RDWP	$(\hat{r}, \hat{q}) = (5.327569, 5.891839)$	$(SE(\hat{r}), SE(\hat{q})) = (3.357067, 3.541312)$
DLD	$\hat{\gamma} = 4.595803$	$SE(\hat{\gamma}) = 0.878736$
PL	$\hat{\nu} = 1.148399$	$SE(\hat{\nu}) = 0.055983$
T-DCD	$\hat{\gamma} = 8.973247$	$SE(\hat{\gamma}) = 1.874255$
T-SDSD	$\hat{\theta} = 0.269590$	$SE(\hat{\theta}) = 0.034322$
T-2SDSD	$(\hat{\theta} = 0.373575, \hat{\beta} = 0.085184)$	$(SE(\hat{\theta}), SE(\hat{\beta})) = (0.069438, 0.291294)$

TABLE 8. ML estimations of the parameters and the corresponding SEs for the fitted models and for the data from [Example 4.2](#)

	ML estimations	SEs
2-RDWP	$(\hat{r}, \hat{q}) = (4.187986, 4.683653)$	$(SE(\hat{r}), SE(\hat{q})) = (1.872645, 1.978388)$
DLD	$\hat{\gamma} = 4.550216$	$SE(\hat{\gamma}) = 0.683555$
PL	$\hat{\nu} = 1.168417$	$SE(\hat{\nu}) = 0.041384$
T-DCD	$\hat{\gamma} = 8.334494$	$SE(\hat{\gamma}) = 1.371416$
T-SDSD	$\hat{\theta} = 0.278301$	$SE(\hat{\theta}) = 0.025886$
T-2SDSD	$(\hat{\theta}, \hat{\beta}) = (0.376976, 0.101890)$	$(SE(\hat{\theta}), SE(\hat{\beta})) = (0.051189, 0.224349)$

As we expected and see in the Tables 7 and 8, for all models (1.2), (5.1), (5.2), (5.3), (5.4) and (5.5), for sample size $n = 105$ the SEs have been reduced with respect to the case $n = 64$.

Moreover, using (2.10) and for the data of Table 1, the asymptotic variance-covariance matrix of the ML estimations for the 2-RDWP model's parameters (r, q) , which is the inverse of the observed Fisher's information matrix, is proposed by

$$(4.2) \quad \mathbf{I}^{-1}(\hat{\alpha}) = \begin{bmatrix} 11.26990 & 11.88401 \\ 11.88401 & 12.54089 \end{bmatrix}$$

From (4.2), we calculate $\det |\mathbf{I}^{-1}(\hat{\alpha})| = 0.104883$. The estimated correlation of \hat{r} and \hat{q} , equals 0.999629.

Again from (2.10) and for the data of Table 3, we have

$$(4.3) \quad \mathbf{I}^{-1}(\hat{\alpha}) = \begin{bmatrix} 3.50680 & 3.70275 \\ 3.70275 & 3.91402 \end{bmatrix}$$

From (4.3), we calculate $\det |\mathbf{I}^{-1}(\hat{\alpha})| = 0.015328$. The estimated correlation of \hat{r} and \hat{q} , equals 0.999441.

Using (2.10), (4.2) and (4.3), we can apply the normal distribution of $\hat{\alpha} = (\hat{r}, \hat{q})$ to construct approximate confidence interval for parameters. In other words, an asymptotic $100(1 - \xi)\%$ confidence interval for the unknown parameters α_i , $i = 1, 2$ ($\alpha_1 = r, \alpha_2 = q$) are given by

$$(\hat{\alpha}_i - z_{\frac{\xi}{2}} \sqrt{\hat{J}_{ii}}, \hat{\alpha}_i + z_{\frac{\xi}{2}} \sqrt{\hat{J}_{ii}})$$

where \hat{J}_{ii} denotes the (i, i) diagonal element of $\mathbf{I}^{-1}(\hat{\alpha})$ and $z_{\frac{\xi}{2}}$ is $(1 - \frac{\xi}{2})$ -th quantile of the standard normal distribution.

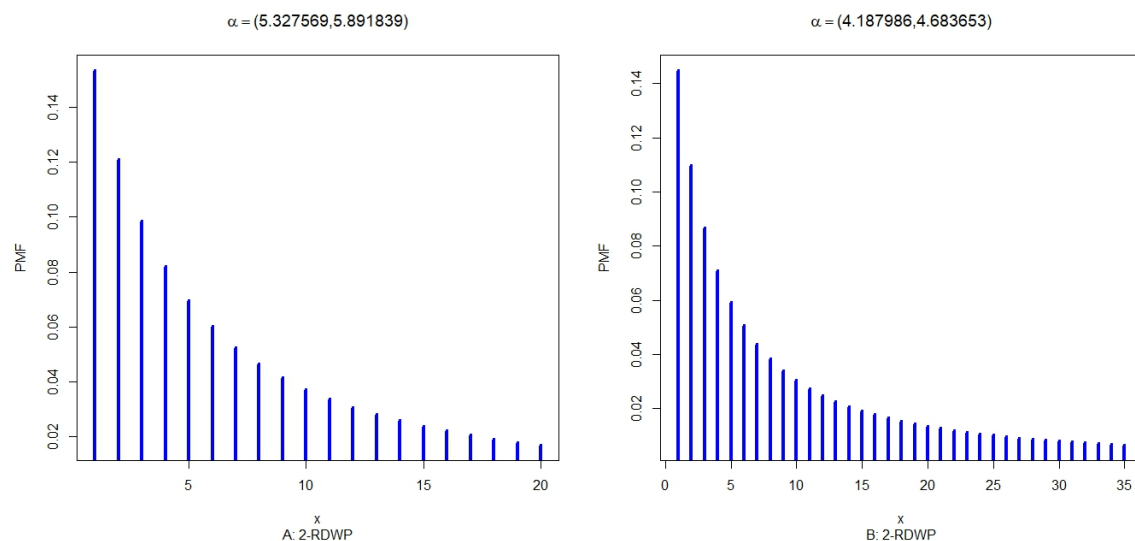


FIGURE 5. Plots of 2-RDWP's PMF based on ML estimations of parameters (\hat{r}, \hat{q}) . A: 2-RDWP for $(\hat{r} = 5.327569, \hat{q} = 5.891839)$, B: 2-RDWP for $(\hat{r} = 4.187986, \hat{q} = 4.683653)$

Remark 2. From Table 7 and based on estimated values $(\hat{r} = 5.327569, \hat{q} = 5.891839)$, we have

$$-\hat{\rho} = -1.56427 < -1.$$

Remark 3. From Table 8 and based on estimated values $(\hat{r} = 4.187986, \hat{q} = 4.683653)$, we have

$$-\hat{\rho} = -1.495667 < -1.$$

Remark 4. All estimated values of parameters (\hat{r}, \hat{q}) (for two real data sets) are satisfied in the condition (1.3). Moreover, for all examples $\hat{r} < \hat{q}$.

5. CONCLUSION

In this research, we considered a skewed regularly varying discrete distribution generated by Waring-type probability, so-called 2-RDWP (1.2). Under satisfying RCs, we established the consistency, asymptotic normality, asymptotic efficiency, and asymptotic unbiasedness of the ML estimators. Some new plots for the CDF, SF, and HRF have been given for different possible values of parameters.

Two real data sets in COVID-19 have been proposed. Using six statistical criteria $(-\ln L, \text{AIC}, \text{AICc}, \text{BIC}, \text{HQIC}, \text{p-value})$, we compared our results for the proposed model (4.1) with five discrete competitive models. For these real data sets, one can conclude that the 2-RDWP model (with two parameters) gives a better fit than other rival models. In the sequel, based on the L-BFGS-B optimization method, ML estimations and SEs of the unknown parameters of the 2-RDWP model and rival models have been obtained.

As an applied result, our 2-RDWP model could be considered not only for modeling biological phenomena [9] but also for modeling medical data such as COVID-19 data sets.

Let us notice that our numerical and computations results have been obtained using *R statistical software* (version 4.3.1).

APPENDIX

We present the PMFs of some rival models, used in Tables 5-8 (DLD, PL, T-DCD, T-SDSD and T-2SDSD).

The PMF of the one-parameter DLD model is given by [7, 11]

$$(5.1) \quad p_x(\gamma) = \frac{x^{-\frac{3}{2}} \exp(-\frac{\gamma}{2x})}{\sum_{y=1}^{\infty} y^{-\frac{3}{2}} \exp(-\frac{\gamma}{2y})}, \quad x = 1, 2, \dots; \quad \gamma > 0.$$

The PMF of the one-parameter PL model is given by [13]

$$(5.2) \quad p_x(\nu) = \frac{x^{-\nu}}{\sum_{y=1}^{\infty} y^{-\nu}}, \quad x = 1, 2, \dots; \quad \nu > 1.$$

The PMF of the one-parameter DCD model truncated at $x = 0$ (say T-DCD) is given by [10]

$$(5.3) \quad f_x(\gamma) = \frac{\left(\frac{\pi^2}{4}\gamma^2 + x^2\right)^{-1}}{\sum_{y=1}^{\infty} \left(\frac{\pi^2}{4}\gamma^2 + y^2\right)^{-1}} \quad x = 1, 2, \dots; \quad \gamma > 0.$$

The PMF of T-SDSD when $0 < \theta < 1$, and $x = 1, 2, \dots$, is given by [8]

$$(5.4) \quad p_x(\theta, 1) = \frac{\Gamma(\theta+1)x^{-\theta-1} \sin(\pi\theta) - \frac{1}{2}\Gamma(2\theta+1)x^{-2\theta-1} \sin(2\pi\theta)}{\sum_{y=1}^{\infty} \left(\Gamma(\theta+1)y^{-\theta-1} \sin(\pi\theta) - \frac{1}{2}\Gamma(2\theta+1)y^{-2\theta-1} \sin(2\pi\theta) \right)}$$

The PMF of T-2SDSD when $0 < \theta < 2$, $0 < \beta \leq 1$, and $x = 1, 2, \dots$, is given by [8]

$$(5.5) \quad p_x(\theta, \beta) = \frac{\Gamma(\theta+1)x^{-\theta-1} \sin\left(\frac{\pi\theta(1+\beta)}{2}\right) - \frac{1}{2}\Gamma(2\theta+1)x^{-2\theta-1} \sin(\pi\theta(1+\beta))}{\sum_{y=1}^{\infty} \left(\Gamma(\theta+1)y^{-\theta-1} \sin\left(\frac{\pi\theta(1+\beta)}{2}\right) - \frac{1}{2}\Gamma(2\theta+1)y^{-2\theta-1} \sin(\pi\theta(1+\beta)) \right)}$$

Acknowledgments The author is grateful to the editor and anonymous referees for their valuable comments and constructive suggestions, which improved the quality of this paper.

REFERENCES

- [1] H. Akaike, *A new look at the statistical model identification*, IEEE Transactions on Automatic Control, **19**(6) (1974), 716–723.
- [2] J. Astola and E. Danielian, *Frequency Distributions in Biomolecular Systems and Growing Networks*, TICSP, Series no. 31, Tampere, Finland, 2007.
- [3] J. Astola, E. Danielian and S. Arzumanyan, *Frequency distributions in bioinformatics*, a review, Proceedings of the Yerevan State University: Physical and Mathematical Sciences, **223**(3) (2010), 3–22.
- [4] A. A. Borovkov, *Mathematical Statistics*, Gordon and Breach Science Publishers, 1998.
- [5] K. P. Burnham and D. R. Anderson, *Model Selection and Multimodel Inference: A practical information-theoretic approach*, 2nd edition, Springer, 2002.
- [6] D. Farbod, *Asymptotic properties of maximum likelihood estimators for a generalized Pareto-type distribution*, Journal of Contemporary Mathematical Analysis, Springer, **50**(1) (2015), 44–51.
- [7] D. Farbod, *Some statistical inferences for two frequency distributions arising in bioinformatics*, Applied Mathematics E-Notes, **14** (2014), 151–160.
- [8] D. Farbod, *Modeling and simulation studies for some truncated discrete distributions generated by stable densities*, Mathematical Sciences, Springer, **16**(2) (2022), 105–114.
- [9] D. Farbod, *On a new regularly varying discrete distribution generated by Waring-type probability*, Journal of Contemporary Mathematical Analysis, Springer, **59**(2) (2024), 96–109.
- [10] D. Farbod and K. V. Gasparian, *Asymptotic properties of maximum likelihood estimator for some discrete distributions generated by Cauchy stable law*, STATISTICA, **68**(3-4) (2008), 321–326.

- [11] D. Farbod and M. Basirat, *On the discrete distribution generated by Levy probability*, Journal of Mathematical Sciences, Springer, **280**(2) (2024), 198–211.
- [12] E. J. Hannan and B. G. Quinn, *The Determination of the Order of an Autoregression*, Journal of the Royal Statistical Society: Series B (Methodological), **41**(2) (1979), 190–195.
- [13] V. A. Kuznetsov, *Distributions associated with stochastic processes of gene expression in a single eukaryotic cell*, EURASIP Journal on Applied Signal Processing, **4** (2001), 258–296.
- [14] V. A. Kuznetsov, A. Grageda and D. Farbod, *Generalized hypergeometric distributions generated by birth-death process in bioinformatics*, Markov Processes and Related Fields, **28**(2) (2022), 303–327.
- [15] G. E. Schwarz, *Estimating the dimension of a model*, Annals of Statistics, **6**(2) (1978), 461–464.
- [16] C. Zhu, R. H. Byrd, P. Lu J. Nocedal, *L-BFGS-B: Algorithm 778: L-BFGS-B, FORTRAN routines for large scale bound constrained optimization*, ACM Transactions on Mathematical Software , **23**(4) (1997), 550–560.
- [17] <https://www.who.int/>
- [18] <https://www.who.int/health-topics/coronavirus>
- [19] <https://www.statista.com/>